

A Rheological and Small-Angle Neutron Scattering Study of the Structure of Gelatin/Polyelectrolyte Complexes under Shear

J. H. E. Hone,[†] A. M. Howe,[‡] and T. Cosgrove*,[†]

School of Chemistry, University of Bristol, Cantock's Close, Bristol BS8 1TS, U.K.; and Kodak European R&D, Headstone Drive, Harrow, Middlesex HA1 4TY, U.K.

Received July 20, 1999; Revised Manuscript Received November 16, 1999

ABSTRACT: The small-angle neutron scattering and rheology of gelatin/polyanion complexes have been studied as a function of shear rate and ionic strength. It was found that the addition of very small amounts of sodium poly(styrene sulfonate) caused a massive increase in the viscosity of gelatin solutions through the formation of a complex between the two net negatively charged polymers. The scattering data showed a maximum in intensity at a specific value of the momentum transfer, reminiscent of the pattern produced by more concentrated pure polyelectrolyte solutions. At high shear rates the complex systems displayed anisotropic behavior: the scattering intensity at the peak was suppressed parallel to the direction of flow, indicating a change in the structure of the complex, but remained approximately constant perpendicular to the flow.

Introduction

Small-angle neutron scattering has been used to study decalcified gelatin solutions in the absence^{1,2} and presence of the anionic surfactant sodium dodecyl sulfate (SDS).^{3–5} These studies have shown that when the scattering length density of the SDS is matched with the solvent, allowing the scattering from the gelatin alone to be observed, the system displays a scattering pattern similar to that seen for (visible) SDS solutions in the absence of gelatin. It has also been shown that there is a significant increase in the viscosity of gelatin solutions upon the addition of SDS,^{6,7} but little shear thinning, within the readily accessible shear rate range, i.e., up to approximately 10^6 s^{-1} .

By way of contrast, the addition of very small quantities of the strong acid polyelectrolytes sodium poly(styrene sulfonate) (NaPSS) or sodium poly(2-acrylamido-2-methylpropane sulfonate) (NaPAMPS) to gelatin solutions produces dramatic increases in the viscosity of the solution and gives highly thixotropic behavior. The ability to thicken and significantly alter the thixotropy of gelatin solutions with a polyelectrolyte of the same net charge, such as NaPSS, has been known since the early 1960s but the mechanism by which these effects are brought about are not well understood. A knowledge of how these two polymers interact under the influence of varying ionic strength and shear will help in discovering the mechanisms behind these association phenomena.

It has been shown through detailed light scattering⁸ and differential size-exclusion chromatography⁹ measurements, that above the isoelectric pH of the gelatin, the polyanion and the net negatively charged gelatin form a relatively strong complex in dilute solution. Surprisingly, it was found that the complexes formed had an effective molecular weight some 12–19 times larger than the parent NaPSS, independent of the molecular weight of the NaPSS, but that the radius of gyration, R_g , of the associated chains was only about 10% greater. It was proposed that the strong interaction

between the like-charged chains was due to the polarization of the gelatin in the presence of the strong electric field of the polyelectrolyte.⁸

As far as we are aware, there has been only one SANS study on the effect of shear on a pure polyelectrolyte solution, by Milas et al.¹⁰ The scattering from high molecular weight xanthan solutions was studied at rest and a shear rate of $12\,000 \text{ s}^{-1}$. They found that when the shear rate was increased, the position of the peak in Q remained constant and the scattering became anisotropic.

Experimental Section

In this work, the polyanion sodium salt poly(styrene sulfonate) was used. Two samples with different molecular weights were used: one with a peak molecular weight of 82.8 kDa supplied by Polymer Standards Service, and one with a peak molecular weight of 780 kDa supplied by Polymer Laboratories Limited. Both had polydispersity indices (M_w/M_n) of 1.1 or less.

All of the samples used for both the rheological and SANS experiments were prepared in D_2O in order to keep the proton content, and therefore the incoherent scattering contribution, to a minimum. All of the percentages quoted are weight-for-weight values. The gelatin used was a fractionated sample¹¹ referred to as α -gelatin because of the abundance of α chains. The α -gelatin had a weight-average molecular weight of 109 kDa and a polydispersity index of 1.42 and was supplied at its IEP, pH 4.9. The ionic strength was altered using sodium acetate supplied by BDH.

Rheological Measurements. A Bohlin VOR rheometer was used in conjunction with two bob-and-cup geometries to measure the viscosity of the samples. A small sample cell geometry (C 2.3/26), was used for measurements over the shear rate range from 0.04 to 2000 s^{-1} and a tapered plug (TP 20:1) geometry for the higher rates (to almost 10^5 s^{-1}). The temperature was kept at $45.0 \pm 0.1^\circ\text{C}$ with a circulating water bath. The instrument was calibrated using an oil (supplied by Poulten, Selfe and Lee) of a known viscosity ($94.36 \text{ mPa}\cdot\text{s}$ at 40.0°C).

SANS Measurements. The SANS data were collected using the LOQ instrument at ISIS, Didcot, Oxfordshire, U.K. The LOQ shear cell¹² was used to obtain the scattering from the NaPSS/gelatin complex both at rest and under shear at $45.0 \pm 0.1^\circ\text{C}$. The shear cell consists of a couette arrangement where the cup is powered by a D.C motor capable of 5000 rpm

[†] University of Bristol.

[‡] Kodak European R&D.

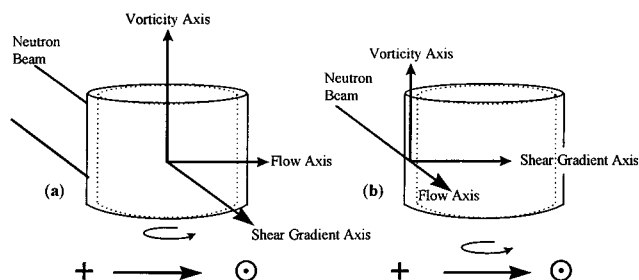


Figure 1. Schematic representation of the LOQ shear cell showing scattering measurements in the vorticity-flow plane (left) and the vorticity-shear gradient plane (right).

equivalent to $\sim 26\,000\text{ s}^{-1}$. The gap between the bob and cup is 0.5 mm giving a total neutron beam path length of 1 mm. Figure 1 shows a schematic representation of the LOQ shear cell and indicates the three mutually perpendicular axes.

Most of the data were recorded with the neutron beam passing through the center of the shear cell, parallel with the shear gradient across the sample (Figure 1a), i.e., in the flow-vorticity plane. One further measurement was made with the shear cell offset to one side so that the beam passed through the edge of the shear cell in the gap between the bob and cup (Figure 1b). This setup enabled the scattering parallel to the direction of flow to be measured as the sample flowed away from the incident radiation; i.e., data were collected in the shear gradient-vorticity plane.

In both cases it is possible to split the LOQ detector into four quadrants as shown in Figure 2. Opposite pairs of quadrants (labeled "A" and "B") record the same scattering information. Most of the measurements were made with the beam passing through the center of the shear cell (Figure 1b) and so the two quadrants labeled "A" refer to scattering occurring in the vorticity-shear gradient plane (perpendicular to the flow) and those labeled "B" refer to scattering from the flow-shear gradient plane (parallel to the flow). For the single measurement made using the shear cell in the offset position (Figure 1b), the quadrants "A" and "B" refer to the scattering in the vorticity-flow plane and the shear gradient-flow plane, respectively.

The scattering data were reduced into plots of scattering intensity against momentum transfer, Q , given by

$$Q = \frac{4\pi}{\lambda} \sin \frac{\theta}{2} \quad (1)$$

where λ is the wavelength of the incident neutron and θ is the scattering angle. This was achieved by radially averaging the scattering data in the relevant pairs of quadrants. The data were then corrected for neutron wavelength, detector efficiency and sample transmission. To obtain absolute scattering cross sections, the scattering from a standard polystyrene copolymer and polystyrene blend were measured and fitted. This procedure provides a scaling factor which is applied to each data set. Scattering data were collected over a Q range from 0.011 to 0.249 \AA^{-1} . Each sample was measured for between 120 and 180 min.

Results and Discussion

First we present the viscosity data as a function of shear rate and shear stress from the polyelectrolyte/ α -gelatin complexes in solution, and then show the scattering from the same samples as a function of applied shear rate.

Rheological Results. The effect of shear on the viscosity of a solution of 5% α -gelatin mixed with 0.3% NaPSS (in D_2O) as a function of molecular weight and ionic strength is shown in Figure 3. The data in Figure 3 have been fitted with the Carreau-Yasuda model

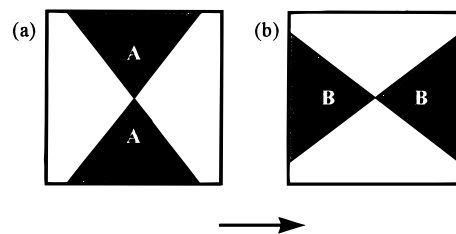


Figure 2. Schematic diagram showing the LOQ area detector split into approximate "quadrants" A and B. The quadrants are radially averaged in pairs in order to analyze anisotropic scattering patterns. The arrow indicates the flow direction.

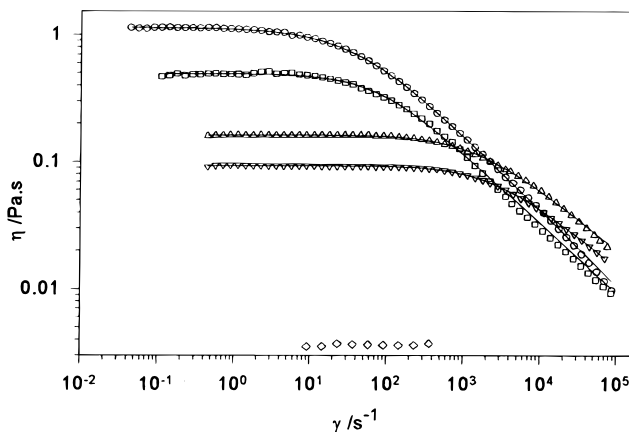


Figure 3. Viscosity vs shear rate at $T = 45\text{ }^{\circ}\text{C}$ for (\diamond) 5% α -gelatin alone and with 0.3% NaPSS; (\circ) 780 kDa no salt; (\square) 780 kDa and 6 mM sodium acetate; (\triangle) 82 kDa no salt; (∇) 82 kDa and 6 mM sodium acetate; (—) Carreau-Yasuda fit.

which is given by

$$\eta(\dot{\gamma}) = \eta(0)(1 + (\lambda\dot{\gamma})^a)^{(n-1)/a} \quad (2)$$

where $\eta(\dot{\gamma})$ is the shear dependent viscosity, $\eta(0)$ is the limiting low-shear Newtonian viscosity, λ is the relaxation time, n is the power-law index, and a describes the transition from the Newtonian regime to the power-law thinning regime. The Carreau model corresponds to $a = 2$. The relaxation time λ is equal to the inverse of the critical shear rate, $\dot{\gamma}_c$, which corresponds to the rate at which the viscosity (given by a power-law fit to the shear thinning regime) is equal to the low-shear Newtonian viscosity. The parameters derived from the fits in Figure 3 are given in Table 1.

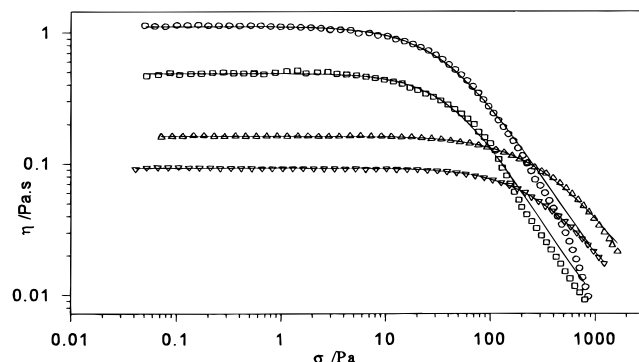
Figure 3 also shows the viscosity of a 5% α -gelatin solution in D_2O at $45\text{ }^{\circ}\text{C}$ with no added NaPSS or salt. The solution has a viscosity of 3.5 mPa·s. On adding 0.3% NaPSS of the high molecular weight polymer, the viscosity increases over 300-fold to more than 1100 mPa·s. This occurs because there is an increase in the effective molecular weight of the polyelectrolyte through the binding of gelatin chains at the concentrations studied here. In contrast dilute solution studies do not show any increase in molecular size.^{8,9}

It is also immediately apparent that all of the mixtures are shear thinning: the viscosity of the 780 kDa NaPSS/ α -gelatin mixture with no added salt decreases by more than 2 orders of magnitude over the measured shear rate range.

The data in Figure 3 have been replotted as viscosity vs shear stress in Figure 4. These data have been fitted

Table 1. Parameters from the Carreau–Yasuda Fits to the Rheological Data in Figure 3, Where $\eta(0)$ Is the Low-shear Viscosity, n Is the Power-law Index, λ Is the Relaxation Time, and a Describes the Transition from the Newtonian to the Power-Law Thinning Regime

sample	$\eta(0)/\text{mPa}\cdot\text{s}$	λ/s	a	n
0.3% 780 kDa NaPSS, 5% α -gelatin, no salt	1138	0.027	0.86	0.41
0.3% 780 kDa NaPSS, 5% α -gelatin, 6 mM sodium acetate	494	0.014	1.11	0.45
0.3% 82 kDa NaPSS, 5% α -gelatin, no salt	163	7.6×10^{-4}	1.02	0.52
0.3% 82 kDa NaPSS, 5% α -gelatin, 6 mM sodium acetate	92.9	4.5×10^{-4}	1.08	0.52

**Figure 4.** Viscosity vs shear stress at $T = 45^\circ\text{C}$ for 5% α -gelatin and 0.3% NaPSS: (○) 780 kDa no salt; (□) 780 kDa and 6 mM sodium acetate; (△) 82 kDa no salt; (▽) 82 kDa and 6 mM sodium acetate; (—) Ellis fit.

with the Ellis model:

$$\eta(\sigma) = \eta(\infty) + \frac{\eta(0) - \eta(\infty)}{1 + (\sigma/\sigma_c)^p} \quad (3)$$

where $\eta(\sigma)$ is the stress dependent viscosity, $\eta(\infty)$ is the high-shear viscosity and p is the exponent which describes the width of the shear thinning regime. At a viscosity halfway between the low- and high-shear viscosities, a critical shear stress, σ_c , can be defined; thus

$$\eta(\sigma_c) = \frac{[\eta(0) + \eta(\infty)]}{2} \quad (4)$$

from the point of view of a colloidal dispersion, σ_c gives the stress at which the applied hydrodynamic force balances with the thermal forces controlling the diffusion of the complex.

The data were fitted by constraining the high-shear viscosity to 3 mPa·s, slightly less than the viscosity of the 5% α -gelatin solution. The derived fitted parameters are shown in Table 2. The model fits the data well at low shear and for the first order of magnitude fall in viscosity. At high shear there is a significant deviation of the data from the model; in particular, the more viscous 780 kDa NaPSS/gelatin complex data have a lower viscosity than anticipated by the model fit. This deviation between the model and the data at high shear may be due to difficulties in obtaining accurate rheological data or due to the deformation or breakdown of the complexes, at such high stresses.

The lower molecular weight NaPSS causes a significant increase in the viscosity of the α -gelatin solution but not to such a large extent as the higher molecular weight sample. This is probably because the complex formed with the lower molecular weight NaPSS is smaller⁸ and therefore the inter-complex overlap is significantly reduced.

The addition of a relatively small quantity of salt to the complexes results in a marked decrease in the solution viscosity. This indicates that electrostatic in-

teractions are of fundamental importance to the structure of the complex. From this small amount of data it is not possible to determine the mechanism by which an increase in the electrolyte concentration influences the rheology. However, it is likely that *both* inter-complex and intra-complex interactions are weakened because of charge shielding. At the same time there may be an increase in the attraction between the gelatin and the NaPSS since hydrophobic interactions may become more significant as the charge interactions are screened.

Therefore, the solution viscosity decreases through both a decrease in the size of the complexes, and a reduction in the amount of complex-complex overlap. Using static light scattering, Bowman et al.⁸ showed that on increasing the ionic strength up to ~ 10 mM sodium acetate there was an increase in the stoichiometry of the complex, but above 10 mM sodium acetate the stoichiometry decreases. However, they also showed that the size of the complex in dilute solution decreases as ionic strength is increased above ~ 3 mM salt, consistent with our rheological data.

Krieger has suggested¹³ that the size of colloidal particles could be obtained by using reduced variables. In particular he introduced the concept of the reduced critical shear stress, σ_{rc} , which gives an indication of the relative importance of the hydrodynamic and Brownian motions in a colloidal suspension, and is given by

$$\sigma_{rc} = \frac{kT}{\sigma_c r_h^3} \quad (5)$$

where k is Boltzmann's constant, T is the absolute temperature and r_h is the hydrodynamic radius of the particle.

Here we have tentatively assumed that the behavior of the individual complex "particles" can be modeled as a dispersion of hard spheres though in reality the system is unlikely to be particulate. However, for a purely qualitative insight, we can derive an effective hydrodynamic radius of the complex from eq 5 provided the value of σ_{rc} is known. Previous studies have found that σ_{rc} is approximately constant for various systems lying in the range 0.1–0.5;^{13–15} here we have used $\sigma_{rc} = 0.3$. The values of σ_c derived from fits to the flow curves in Figure 4 are given in Table 2. The derived hydrodynamic radii of the complexes are given in Table 3.

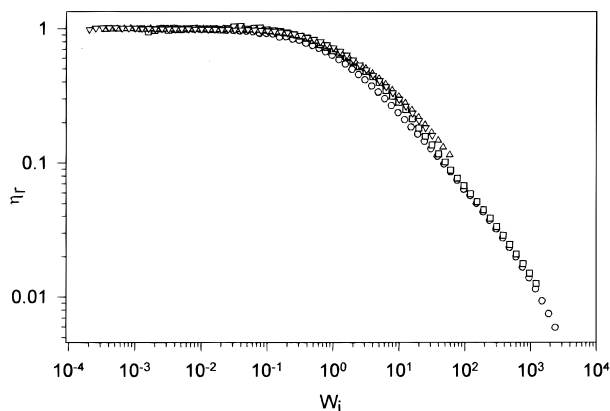
Despite the rather tenuous use of eq 5, originally derived for the analysis of rheological data from colloidal systems, there is good agreement between the hydrodynamic complex radii measured by rheology and the sizes found by Bowman et al. using light scattering.⁸ The rheology gives a hydrodynamic radius of 660 Å for 780 kDa NaPSS/ α -gelatin complex (at 45°C , pH 5.9, and 6 mM sodium acetate), which compares well with 700 Å for dilute 1090 kDa NaPSS/gelatin complexes (at 40°C , pH 5.65 and 10 mM sodium acetate⁸) cf. $R_g \approx$

Table 2. Parameters from the Ellis Model Fits to the Rheological Data in Figure 4, Where $\eta(0)$ and $\eta(\infty)$ Are the Low- and High-Shear Viscosities Respectively, p Is the Width of the Shear Thinning Regime, and σ_c Is the Critical Shear Stress

sample	$\eta(0)/\text{mPa}\cdot\text{s}$	$\eta(\infty)/\text{mPa}\cdot\text{s}$	p	σ_c/Pa
0.3% 780 kDa NaPSS, 5% α -gelatin, no salt	1117	3	1.267	39.2
0.3% 780 kDa NaPSS, 5% α -gelatin, 6 mM sodium acetate	491	3	1.393	46.9
0.3% 82 kDa NaPSS, 5% α -gelatin, no salt	162	3	1.175	338
0.3% 82 kDa NaPSS, 5% α -gelatin, 6 mM sodium acetate	92.7	3	1.236	330
5% α -gelatin, no salt	3.5			

Table 3. Complex Radii Derived from the Flow Curves in Figure 4 (Assuming $\sigma_{rc} = 0.3$)

sample	σ_c/Pa	$r_h/\text{\AA}$
0.3% 780 kDa NaPSS, 5% α -gelatin, no salt	39.2	700
0.3% 780 kDa NaPSS, 5% α -gelatin, 6 mM sodium acetate	46.9	660
0.3% 82 kDa NaPSS, 5% α -gelatin, no salt	338	342
0.3% 82 kDa NaPSS, 5% α -gelatin, 6 mM sodium acetate	330	344

**Figure 5.** Master rheology curve showing reduced viscosity vs Weissenberg number for 5% α -gelatin gelatin and 0.3% NaPSS: (○) 780 kDa no salt; (□) 780 kDa and 6 mM sodium acetate; (△) 82 kDa no salt; (▽) 82 kDa and 6 mM sodium acetate. $T = 45^\circ\text{C}$.

550 \AA for 780 kDa in 0.1 M NaCl¹⁶ and 380 \AA for 77 kDa in 0.1 M NaCl.¹⁶

Using the principle of reduced variables, it is possible to replot the viscosity vs shear rate data in Figure 4 in terms of a relative viscosity, η_r , against the Weissenberg number, W_i , which are given by

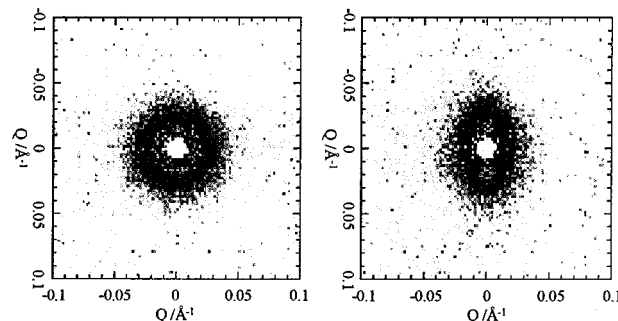
$$\eta_r = \frac{\eta(\dot{\gamma})}{\eta(0)}$$

$$W_i = \dot{\gamma}\lambda \quad (6)$$

respectively. This plot is shown in Figure 5.

All of the data collapse reasonably well onto a master curve. The flow curves for all of the systems now have a normalized low-shear viscosity and begin to thin at the same reduced shear rate (W_i) of about 0.3. Above $W_i = 0.3$, the curves begin to shear thin, with the power-law thinning behavior being fully developed by $W_i \approx 5$. Expressing the rheology data in terms of relative viscosity and Weissenberg number for the different solutions facilitates greatly the comparison of the effect of shear experienced at a given rate.

SANS Results. It has been shown in the accompanying paper¹⁷ that the scattering from mixtures of solutions of anionic polyelectrolyte and α -gelatin above its IEP give rise to a scattering pattern reminiscent of that from pure polyelectrolyte solutions. As for pure polyelectrolyte solutions, we have observed a peak in the

**Figure 6.** Scattering pattern from 0.3% 780 kDa NaPSS/5% α -gelatin in D_2O at rest (top) and at 20 000 s^{-1} (bottom) measured in the flow-vorticity plane (Figure 1a). $T = 45^\circ\text{C}$.

scattering labeled Q^* . In this work, we investigate the effect of a shearing force on the scattering from the solution, in particular the scattering intensity and the position of Q^* , at various points on the flow curve.

Figure 6 shows the scattering pattern observed on the LOQ detector for the 0.3% 780 kDa NaPSS/5% α -gelatin sample both at rest and under high shear. At rest, there is a peak in the scattering at $Q \approx 0.02 \text{ \AA}^{-1}$; the application of a shear rate of 20 000 s^{-1} results in anisotropic scattering. The scattering patterns in Figure 6 are very similar to the patterns observed by Milas et al. on shearing a more concentrated solution of pure polyelectrolyte.¹⁰

Before studying the scattering from the complexes in solution in detail, it is important to note, although the data have not been shown here, that the scattering from a 5% α -gelatin solution in D_2O did not show any anisotropy when sheared at 10 000 s^{-1} . Since there is no structure peak in the gelatin scattering,¹⁻⁵ anisotropy would not be expected, particularly at only 10 000 s^{-1} , since more concentrated pure gelatin solutions (15% w/w) do not show any thixotropic behavior until shear rates in excess of 10 000 s^{-1} .^{18,19} A similar experiment on a 0.3% NaPSS solution in D_2O was also performed, however it was not possible to discern any anisotropy because the scattering intensity was too weak.¹⁷ It was found, however, that when the sample was removed from the couette cell, after being sheared at 10 000 s^{-1} for 140 min, that it appeared cloudy, as if the NaPSS had precipitated. Since the sample has a low viscosity, similar to that of water, and the shear rate was reasonably high, there may have been Taylor vortices present in the couette, however, this does not necessarily explain the visible degradation of the sample.

To display this anisotropy in plots of $I(Q)$ vs Q , the data on the detector have been split into two areas (approximate 90° quadrants) that separate the scattering from regions of the sample travelling "parallel" to the flow direction and those travelling "perpendicular" to the flow.

Figure 7 shows the $I(Q)$ vs Q plot for the scattering from 0.3% 82 kDa NaPSS/5% α -gelatin in D_2O at rest and at two rates of shear, just below the reciprocal of

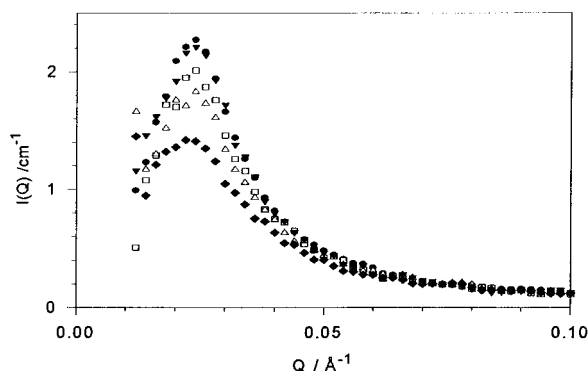


Figure 7. Scattering from 0.3% 82 kDa NaPSS/5% and 5% α -gelatin: (●) at rest; (□) perpendicular and (△) parallel at 1000 s^{-1} , $W_i = 0.76$; (▼) perpendicular and (◆) parallel at $10\,000 \text{ s}^{-1}$, $W_i = 7.6$. $T = 45^\circ\text{C}$.

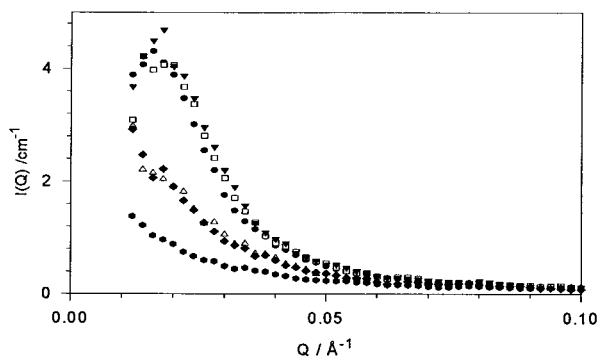


Figure 8. Scattering from 0.3% 780 kDa NaPSS/5% and 5% α -gelatin: (●) at rest; (□) perpendicular and (△) parallel at 5000 s^{-1} , $W_i = 134$; (▼) perpendicular and (◆) parallel at $20\,000 \text{ s}^{-1}$, $W_i = 546$. $T = 45^\circ\text{C}$. Also shown in the lowest curve (●) is a sample of 5% α -gelatin alone.

the relaxation time (1000 s^{-1}) and at the onset of power-law behavior ($10\,000 \text{ s}^{-1}$).

At the high shear rate ($10\,000 \text{ s}^{-1}$) there is appreciable anisotropy. Parallel to the direction of the shear, the scattering is reduced (although the peak is still visible), while perpendicular to the flow the scattering is approximately the same as the scattering from the system at rest. The degree of anisotropy, for this sample, appears to be shear dependent. The position of Q^* in both the parallel and perpendicular direction is independent of the shear rate. This invariance of Q^* under shear has been observed for more concentrated pure polyelectrolyte solutions.¹⁰

The decrease in the scattering intensity in the direction of the flow can be explained qualitatively by the stretching of the coils by the shear field giving an increase in the size in the direction of the flow. An increase in size would cause the form factor to decrease more rapidly at low Q . If, as a first approximation, we assume that the "structure factor" is unaltered by shear, then a decrease in scattering intensity at low Q should be observed.

Figure 8 shows the reduced $I(Q)$ vs Q plot for the 0.3% 780 kDa NaPSS/5% α -gelatin complex at rest, at 5000 s^{-1} and at $20\,000 \text{ s}^{-1}$. The scattering from the complex formed with this particular NaPSS molecular weight is different from the 82 kDa sample in Figure 7, being more intense and having a peak at lower Q .

It was thought that the variation in the expected position of Q^* (predicted from the previous observation¹⁷ that $Q^* \sim c_p^{1/2}$) and of the change in scattering intensity,

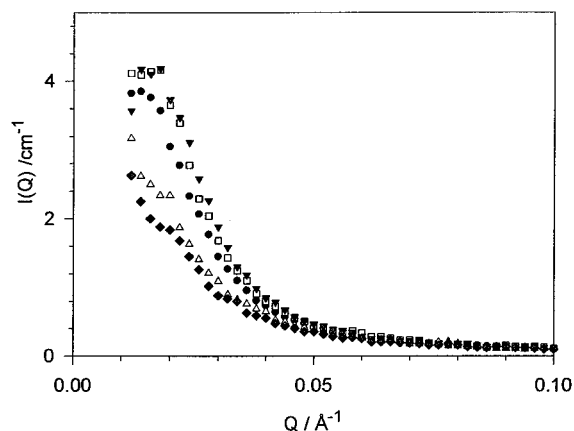


Figure 9. Scattering from 0.3% 82 kDa NaPSS/5%, 5% α -gelatin, and 6 mM sodium acetate, at $T = 45^\circ\text{C}$: (●) at rest; (□) perpendicular and (△) parallel at 1000 s^{-1} , $W_i = 0.45$; (▼) perpendicular and (◆) parallel at $10\,000 \text{ s}^{-1}$, $W_i = 4.5$.

were probably a result of contamination by ionic species of this particular NaPSS sample. However, the specific position of Q^* does not affect the general conclusions which can be drawn from the effect of shear.

In Figure 8, the shear rates used were much larger to see if a more pronounced anisotropy would be displayed at higher rates. However, the same scattering patterns parallel and perpendicular to the flow are seen at both the lower (5000 s^{-1}) and the higher shear rate ($20\,000 \text{ s}^{-1}$).

At first there appears to be a discrepancy between the degree of anisotropy observed for the two different samples, the 82 kDa complex showing a gradual increase in the degree of anisotropy, while the anisotropy displayed by the 780 kDa complex is shear independent. However, close inspection of the reduced rheological data in Figure 5 shows that for the high molecular weight complex, both the low and high shear rates (corresponding to Weissenberg numbers of 134 and 546) are well into the shear thinning regime. In contrast, for the 82 kDa complex, the low shear rate ($W_i = 0.76$) corresponds to the transition region between Newtonian and shear thinning behavior, while the high shear rate ($W_i = 7.6$), is again definitely in the shear thinning regime.

It seems that as the applied shear is increased from the Newtonian region, the degree of anisotropy rises until some critical reduced shear rate, when the anisotropy becomes shear rate independent once again. This supposition also holds for the scattering data from the samples with 6 mM sodium acetate added.

Figures 9 and 10 show that scattering from the 82 kDa and 780 kDa complexes in 6 mM sodium acetate, respectively. As seen before for pure polyelectrolyte solutions^{20,21} and NaPSS/ α -gelatin complexes,¹⁷ the peak in the scattering moves to lower Q .

The effects of shear are less clear when small amounts of salt have been added to the system. To highlight the degree of anisotropy in the scattering, $\Delta I_{\text{aniso}}(Q)$, as shear is applied the data in Figures 9 and 10 have been replotted as the difference between the scattering in both parallel $I_{\parallel}(Q)$ and perpendicular $I_{\perp}(Q)$ directions (at both shear rates) from the static scattering $I_{\text{static}}(Q)$, i.e.

$$\Delta I_{\text{aniso}}(Q) = I_{\parallel,\perp}(Q) - I_{\text{static}}(Q) \quad (7)$$

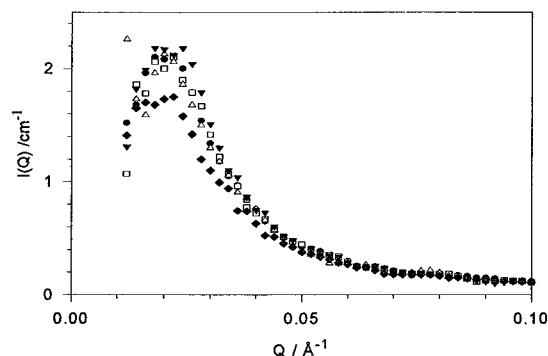


Figure 10. Scattering from 0.3% 780 kDa NaPSS/5%, 5% α -gelatin, and 6 mM sodium acetate, at $T = 45^\circ\text{C}$: (●) at rest; (□) perpendicular and (△) parallel at 1000 s^{-1} , $W_i = 14.2$; (▼) perpendicular and (◆) parallel at $10\,000\text{ s}^{-1}$, $W_i = 142$.

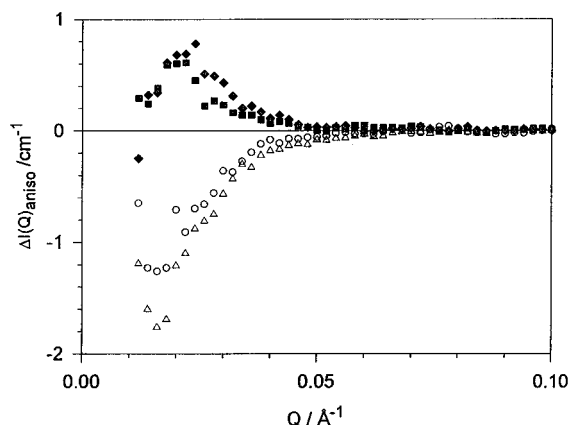


Figure 11. Scattering anisotropy vs Q for 5% α -gelatin, 0.5% 780 kDa NaPSS, in 6 mM sodium acetate at 1000 s^{-1} and $W_i = 14.2$: (○) parallel; (■) perpendicular. At $10\,000\text{ s}^{-1}$ and $W_i = 142$: (△) parallel; (◆) perpendicular.

The scattering anisotropy for the 780 kDa complex in 6 mM salt is shown in Figure 11. In this plot positive values show an increase in anisotropy with respect to the static scattering curve and negative values a decrease in anisotropy. At 1000 s^{-1} there is a decrease in the anisotropy in the parallel direction and an increase in the perpendicular direction. As the shear rate increases to $10\,000\text{ s}^{-1}$ ($W_i = 142$) the anisotropy in the perpendicular direction remains approximately constant, but in the parallel direction the degree of anisotropy decreases further, presumably through the further loss of order as the shear rate increases.

Figure 12 shows the degree of loss of anisotropy in the parallel direction for each sample. It can be seen that as the Weissenberg number increases (and hence the relative viscosity decreases), the loss of anisotropy increases. The anisotropy ceases to decrease (see Figure 12d), once the shear rate corresponds to the power-law thinning regime. At this point the chains are as disoriented by the shear flow as is possible, and further increases in shear rate cause no further changes in structure.

One final data set measured under shear (Figure 13) is rather different from those shown above. As described in the Experimental Section, the scattering has been measured with the shear cell offset and therefore with the direction of the flow parallel to the neutron beam. Now the direction labeled "parallel" shows the scattering from the sample across the shear gradient, but the direction labeled "perpendicular" remains at right-

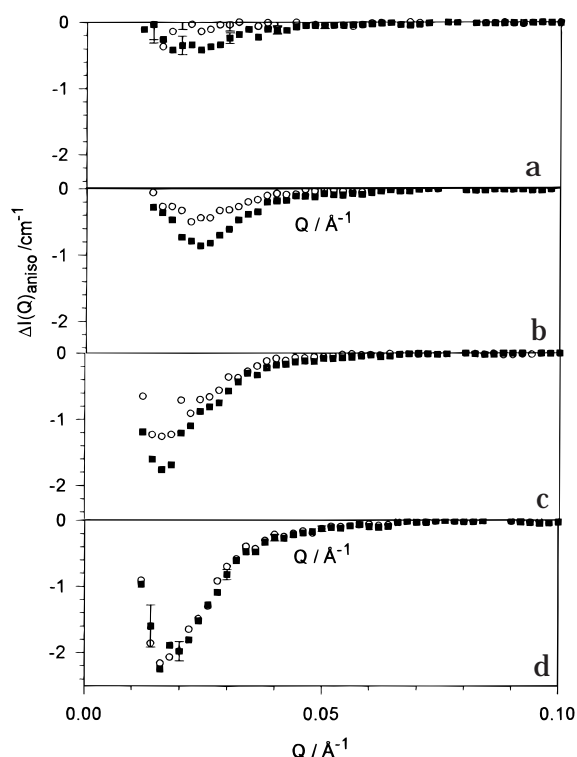


Figure 12. Scattering anisotropy vs Q . (a) 5% α -gelatin, 0.5% 82 kDa NaPSS, in 6 mM sodium acetate: (○) 1000 s^{-1} and $W_i = 0.45$; (■) $10\,000\text{ s}^{-1}$ and $W_i = 4.5$. (b) 5% α -gelatin and 0.5% 82 kDa NaPSS: (○) 1000 s^{-1} and $W_i = 0.76$; (■) $10\,000\text{ s}^{-1}$ and $W_i = 7.6$. (c) 5% α -gelatin, 0.5% 780 kDa NaPSS, in 6 mM sodium acetate: (○) 1000 s^{-1} and $W_i = 14.2$; (■) $10\,000\text{ s}^{-1}$ and $W_i = 142$. (d) 5% α -gelatin and 0.5% 780 kDa NaPSS: (○) 5000 s^{-1} and $W_i = 135$; (■) $20\,000\text{ s}^{-1}$ and $W_i = 542$.

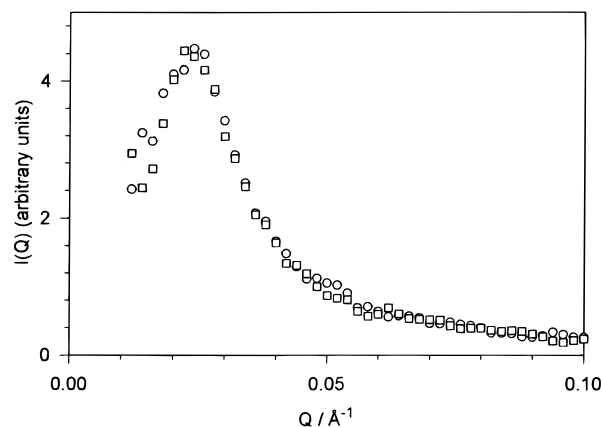


Figure 13. End-on scattering of 0.3% 82 kDa NaPSS/5% α -gelatin in D_2O , at 45°C , $\dot{\gamma} = 10\,000\text{ s}^{-1}$: (○) parallel; (□) perpendicular.

angles to the flow (see Figure 1). The scattering is not displayed on an absolute scale because, with the shear cell in this configuration, it is not possible to exactly determine the neutron path length.

The end-on scattering shows no anisotropy in contrast to the data shown in Figure 13 for the same sample, but measured in the conventional way, through the center of the shear cell. The implication is that there is no measurable deformation (with respect to the static structure) in the polyelectrolyte–gelatin complex in the shear gradient direction nor in the direction perpendicular to the flow (as described above for most of the samples). It would appear that the scattering is only

suppressed in the direction of the flow, presumably as a result of a significant change in the conformation of the complex and therefore the supporting polyelectrolyte chain.

Conclusions

Rheological and SANS measurements have been performed on mixtures of NaPSS and α -gelatin with and without added salt. It has been shown here and previously^{8,9} that the two polymers bind together resulting in a large increase in solution viscosity. The solutions are highly thixotropic at shear rates much lower than those required to thin pure gelatin solutions. The SANS curves show a maximum in intensity, a feature characteristic of pure polyelectrolyte solutions. The peak has been found to be insensitive to NaPSS molecular weight.

Increasing the salt concentration screens the charges in the system, increasing the scattering at low Q and moving the peak to lower Q . This is also in agreement with the work of others on pure polyelectrolyte solutions.^{20,21}

Shearing the NaPSS/ α -gelatin solutions was found to produce anisotropic scattering. Perpendicular to the direction of flow the scattering pattern was unaltered, but parallel to the flow there was a reduction in the scattering intensity, and at very high shear there was a complete loss of the scattering peak. The degree to which anisotropy was observed, was found to be related to the degree of shear thinning of the sample. This indicates that there is a significant change in the structure of the complex in the direction of the flow which is reflected by the change in the macroscopic viscosity of the solution.

Acknowledgment. We are very grateful to Dr. Tom Whitesides, Eastman Kodak Company, Rochester, NY, for preparing the α -gelatin and supplying the accompanying analytical data. We would like to thank Dr. Steve King for help with the shear cell on LOQ and ISIS for providing the beamtime. J.H.E.H. acknowledges

Kodak European Research and Development and the EPSRC for funding.

References and Notes

- (1) Pezron, I.; Herning, T.; Djabourov, M.; Leblond, J. In *Physical Networks: Scattering from a Biopolymer Solution in Sol and Gel States: The Gelatin Example*; Burchard, W., Ross-Murphy, S. B., Eds.; Elsevier Applied Science: London and New York, 1990.
- (2) Pezron, I.; Djabourov, M.; Leblond, J. *Polymer* **1991**, *32*, 3201.
- (3) Cosgrove, T.; White, S. J.; Zerbakhsh, A.; Heenan, R. K.; Howe, A. M. *J. Chem. Soc., Faraday Trans.* **1996**, *92*, 595.
- (4) Cosgrove, T.; White, S. J.; Zerbakhsh, A.; Heenan, R. K.; Howe, A. M. *Langmuir* **1995**, *11*, 744.
- (5) Heenan, R. K.; White, S. J.; Cosgrove, T.; Zerbakhsh, A.; Howe, A. M.; Blake, T. D. *Prog. Colloid Polym. Sci.* **1994**, *97*, 316.
- (6) Greener, J.; Contestable, B. A.; Bale, M. D. *Macromolecules* **1987**, *20*, 2490.
- (7) Howe, A. M.; Wilkins, A. G.; Goodwin, J. W. *J. Photogr. Sci.* **1992**, *40*, 234.
- (8) Bowman, W. A.; Rubinstein, M.; Tan, J. S. *Macromolecules* **1997**, *30*, 3262.
- (9) Tan, J. S.; Harrison, C. A.; Li, J. T.; Caldwell, K. D. *J. Polym. Sci., Part B: Polym. Phys.* **1998**, *36*, 537.
- (10) Milas, M.; Lindner, P.; Rinaudo, M.; Borsali, R. *Macromolecules* **1996**, *29*, 473.
- (11) Griffiths, P. C.; Stilbs, P.; Howe, A. M.; Whitesides, T. H. *Langmuir* **1996**, *12*, 5302.
- (12) Cummins, P. G.; Staples, E.; Millen, B.; Penfold, J. *Meas. Sci. Technol.* **1990**, *1*, 179.
- (13) Krieger, I. M. *Adv. Colloid Interface Sci.* **1972**, *3*, 111.
- (14) Jones, D. A. R.; Leary, B.; Boger, D. *J. Colloid Interface Sci.* **1991**, *147*, 479.
- (15) Hone, J. H. E.; Howe, A. M.; Whitesides, T. H. *Colloids Surf.* **1999**, in press.
- (16) Obey, T. M. Ph.D. Thesis, University of Bristol, 1987.
- (17) Hone, J. H. E.; Howe, A. M.; Cosgrove, T. *Macromolecules* **2000**, *33*, 1206.
- (18) Eastman, J. R. Ph.D. Thesis, University of Bristol, 1996.
- (19) Turner, R. J. Personal communication, 1998.
- (20) Ise, N.; Okubo, T.; Kunugi, S.; Matsuoka, H.; Yamamoto, K.; Ishii, Y. *J. Chem. Phys.* **1984**, *81*, 3294.
- (21) Moussaid, A.; Schosseler, F.; Munch, J. P.; Candau, S. J. *J. Phys II* **1993**, *3*, 573.

MA9911748